Nonreciprocal acoustic transmission in cascaded resonators via spatiotemporal modulation

Chen Shen,* Junfei Li, Zhetao Jia, Yangbo Xie, and Steven A. Cummer†
Department of Electrical and Computer Engineering, Duke University, Durham, North Carolina 27708, USA

(Received 11 December 2018; revised manuscript received 9 April 2019; published 22 April 2019)

Systems that break transport reciprocity have recently opened exciting possibilities for wave manipulation. Here we report nonreciprocal acoustic transmission in cascaded resonators that are modulated in space and time. An analytic approach is developed and the design strategy is discussed for realizing a physical system based on this approach. The theory is verified numerically by finite-difference time-domain (FDTD) simulations, with a one-way isolation factor greater than 25 dB out of just two resonators. Our work provides a feasible route to achieve nonreciprocal acoustic transmission in a compact manner.

DOI: 10.1103/PhysRevB.99.134306

I. INTRODUCTION

Reciprocity is a fundamental constraint in wave dynamics: the transmission from one point to another remains unchanged when the positions of the two points are switched. Breaking reciprocity offers rich possibilities in controlling wave transport and wave-matter interaction, and is highly desired in a number of applications, such as sensing and communication, imaging, and signal processing. In electromagnetism and optics, nonreciprocity has been demonstrated through a number of means, including use of magnetic materials [1], breaking time-reversal symmetry [2], and creating topological effects [3,4]. While recent years have witnessed a growing research interest of nonreciprocal photonics, nonreciprocity within the field of acoustics is largely unexplored [5].

One possible approach to achieve acoustic nonreciprocity is to use passive or active nonlinearity that converts the energy of the fundamental frequency component to higher harmonics [6–9]. Although the isolation factor in principle can be very high, such approaches typically require complicated systems, can be challenging to model accurately, and will inevitably induce signal distortion. Moreover, the intensity of the input signals often needs to be strong to induce nonlinear effects. Other successful strategies include use of topological insulators that break time-reversal symmetry [10–12]. However, these systems are often realizable only with complex and relatively bulky structures.

Recently, nonreciprocal devices based on spatiotemporal modulation have gained significant research interest in different physical systems [2,13–23]. Time-reversal symmetry is broken in time-modulated systems and therefore nonreciprocity can be achieved. In principle, time-modulated devices can be compact and still exhibit strong nonreciprocity. The modulation frequency, modulation depth, geometry of the unit cells, and other parameters provide many degrees of freedom to realize a range of functionalities and performance.

In this paper we propose and analyze nonreciprocal acoustic transmission based on cascaded, spatiotemporally modulated resonators. Although the basic approach is general, we consider here a one-dimensional (1D) propagation scenario, in which Helmholtz resonators are connected to a host waveguide and, through dynamic modulation of the volume of the cavities, one-way transport of acoustic waves can be achieved. An analytic model is developed to characterize the transmission behavior of the system. It is shown that by applying a spatially varying phase difference between the resonators, strong nonreciprocity can be created. The isolation factor can reach more than 25 dB with easily realizable modulation parameters using only two resonators. The relative parameters are discussed and a practical realization of the system is proposed, with its size being approximately a quarter wavelength. FDTD simulations with actual geometrical parameters and time-varying boundary conditions are provided to verify the nonreciprocal effect.

II. THEORY

We begin by considering a simple modulated resonator system, namely a 1D acoustic waveguide with two cascaded Helmholtz resonators loaded on the side, as shown in Fig. 1. The propagation direction of the acoustic waves is along the x direction. The background medium is a linear isotropic fluid (i.e., air or water) with density ρ_0 and speed of sound c_0. The incident, reflected, and transmitted acoustic waves are denoted as p_i, p_r, and p_t, respectively. For an incident wave with pressure p_0 and wave vector k, the acoustic waves inside the waveguide can be expressed as summation of different orders:

$$\begin{aligned} p_i(x) &= p_0 e^{j(\omega t - kx)}, \\ p_r(x) &= \sum_n r_n p_0 e^{j(\omega_n t + k_n x)}, \\ p_t(x) &= \sum_n t_n p_0 e^{j[\omega_n t - k_n (x-d)]}, \end{aligned} \tag{1}$$

where r_n and t_n are the reflection and transmission associated with the nth mode, and d is the distance between the two resonators. Under time modulation, the harmonics ω_n are given

*chen.shen4@duke.edu
†cummer@ee.duke.edu

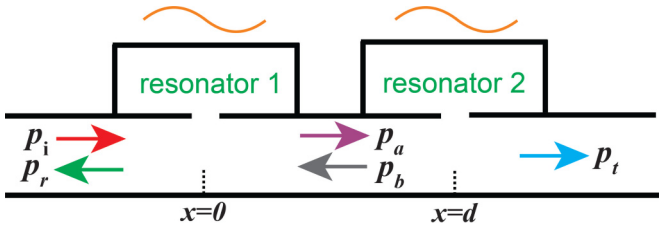

FIG. 1. Sketch of the transmission through a two cascaded resonator system with spatiotemporal modulation. The distance between the resonators is d and only 1D wave propagation is considered.

as $\omega_n = \omega + n\Omega$ with Ω being the modulation frequency. The wave vector with the nth mode can therefore be expressed as $k_n = \omega_n/c_0$. The pressure field in between the two resonators is also a summation of various harmonics of forward and backward waves with coefficients a_n and b_n:

$$p_a(x) = \sum_n a_n p_0 e^{j(\omega_n t - k_n x)},$$
$$p_b(x) = \sum_n b_n p_0 e^{j(\omega_n t + k_n x)}. \tag{2}$$

The resonators loaded on the side of the waveguide can be characterized by resonance frequency $\omega_0 = 2\pi f_0$. We do not restrict ourselves to a specific type of resonators but instead introduce a quality factor Q to describe the overall performance by considering the effect of the waveguide. It will be shown that the overall quality factor of the entire system, i.e., side-loaded resonators together with the host waveguide, is a more important metric to characterize the scattering parameters of the system. Its renormalized impedance, when loaded in the waveguide, is written as $Z = j\omega M_0 + 1/j\omega C_0$, with $M_0 = Z_0 Q/2\omega_0$ and $C_0 = 2/Z_0 Q\omega_0$. In practice, for a side-loaded Helmholtz resonator, the renormalized impedance can be computed by considering the cross-sectional areas of the waveguide and the neck of the resonator [24]. Both resonators are subject to temporal modulation in a fashion that the capacitance can be written as

$$\frac{1}{j\omega C_{1,2}(t)} = \frac{1}{j\omega C_0}[1 + m\cos(\Omega t - \phi_{1,2})]. \tag{3}$$

Here m is modulation depth, and $\phi_{1,2}$ is the initial phase of the modulation. By recognizing that $\rho_0 \frac{\partial \vec{v}}{\partial t} = -\nabla p$, the corresponding acoustic velocity fields can be obtained (note that only 1D wave propagation is considered):

$$\vec{v}_i(x) = \frac{k_x}{\omega\rho_0} p_0 \hat{x} e^{j(\omega t - kx)},$$
$$\vec{v}_r(x) = -\sum_n \frac{k_n}{\omega_n \rho_0} r_n p_0 \hat{x} e^{j(\omega_n t + k_n x)},$$
$$\vec{v}_t(x) = \sum_n \frac{k_n}{\omega_n \rho_0} t_n p_0 \hat{x} e^{j[\omega_n t - k_n (x-d)]}, \tag{4}$$
$$\vec{v}_a(x) = \sum_n \frac{k_n}{\omega_n \rho_0} a_n p_0 \hat{x} e^{j(\omega_n t - k_n x)},$$
$$\vec{v}_b(x) = -\sum_n \frac{k_n}{\omega_n \rho_0} b_n p_0 \hat{x} e^{j(\omega_n t + k_n x)}.$$

At $x = 0$, continuity of pressure yields

$$p_0 e^{j\omega t} + \sum_n r_n p_0 e^{j\omega_n t} = \sum_n a_n p_0 e^{j\omega_n t} + \sum_n b_n p_0 e^{j\omega_n t}. \tag{5}$$

Equation (5) holds for arbitrary t, and can be simplified as

$$\delta_n + r_n = a_n + b_n, \tag{6}$$

where δ_n is the Kronecker delta. On the other hand, the velocity field and the acoustic pressure at $x = 0$ can be related by the surface acoustic impedance, i.e., $Z_a(v_i + v_r - v_a - v_b)$ $S_w/S_H = p\,|_{x=0}$, where S_w and S_H are the cross-sectional areas of the waveguide and the neck of the Helmholtz resonator, respectively. Again, we note that the term S_w/S_H is absorbed in the renormalized impedance Z for convenience. Under dynamic modulation outlined by Eq. (3), the impedance at the site of the first resonator $Z_1(t)$ at ω_n is written as

$$Z_1(t) = Z_n + \frac{mZ_{cn}}{2}[e^{j(\Omega t - \phi_1)} + e^{-j(\Omega t - \phi_1)}], \tag{7}$$

where $Z_n = j\omega_n M_0 + 1/j\omega_n C_0$ and $Z_{cn} = 1/j\omega_n C_0$. The following equation can be obtained by inserting Eqs. (6) and (7) into the impedance relation:

$$\begin{aligned} &2\delta_n \frac{Z_n}{z_0} e^{j\omega_n t} + \left(m\delta_{n-1}\frac{Z_{cn-1}}{z_0} e^{-j\phi_1} + m\delta_{n+1}\frac{Z_{cn+1}}{z_0} e^{j\phi_1}\right) e^{j\omega_n t} \\ &-2\frac{Z_n}{z_0} a_n e^{j\omega_n t} - m\frac{Z_{cn-1}}{z_0} e^{-j\phi_1} a_{n-1} e^{j\omega_n t} - m\frac{Z_{cn+1}}{z_0} e^{j\phi_1} a_{n+1} e^{j\omega_n t} \\ &= a_n e^{j\omega_n t} + b_n e^{j\omega_n t}, \end{aligned} \tag{8}$$

where $z_0 = \rho_0 c_0$ is the free space impedance. Let $A_n = 2Z_n/z_0 + 1$ and $B_n = Z_{cn}/z_0$, Eq. (8) can be further simplified as

$$\begin{aligned} &A_n a_n + mB_{n-1}a_{n-1}e^{-j\phi_1} + mB_{n+1}a_{n+1}e^{j\phi_1} - 2\delta_n \frac{Z_n}{z_0} \\ &- m\delta_{n-1}B_{n-1}e^{-j\phi_1} - m\delta_{n+1}B_{n+1}e^{j\phi_1} + b_n = 0. \end{aligned} \tag{9}$$

Following the same procedure, another difference equation can be established at $x = d$:

$$\begin{aligned} &A_n b_n e^{jk_n d} + mB_{n-1}b_{n-1}e^{jk_{n-1}d}e^{-j\phi_2} \\ &+ mB_{n+1}b_{n+1}e^{jk_{n+1}d}e^{j\phi_2} + a_n e^{-jk_n d} = 0. \end{aligned} \tag{10}$$

Under the condition of weak modulation, i.e., m is much smaller than 1, the coupling from fundamental mode to higher order harmonics ($|n| \geqslant 3$) is low, and only $n = 0, \pm 1, \pm 2$ needs to be considered in Eq. (10). A series of difference equations can be established and the coefficients of a_n and b_n can be calculated. Finally, the transmission of the system can be analyzed by using the continuity of pressure at $x = d$, which yields

$$t_n = a_n e^{-jk_n d} + b_n e^{jk_n d}. \tag{11}$$

We first study the transmission characteristics of the cascaded resonator system. Choosing physically reasonable parameters, we assume the resonators are characterized by a resonance frequency of $f_0 = 2000$ Hz and quality factor $Q = 3.6$. In practice, the quality factor of the resonators can be conveniently tuned by adjusting the height of the waveguide while keeping the size of the resonator unchanged. The

distance d between the two resonators is 4.29 cm, which is a quarter wavelength at the frequency of 2000 Hz. This distance is selected for the sake of compactness of the system. In general, the modulation strategy can be optimized at different distances to display nonreciprocal effects. Since the initial phase difference creates a temporal bias that breaks the time invariance of the system, we choose $\Delta\phi = |\phi_1 - \phi_2| = 0.4\pi$ to induce a sufficiently large asymmetry in opposite directions. The temporal modulation frequency is chosen to be $\Omega = 0.125\omega_0$, where $\omega_0 = 2\pi f_0$, so that different harmonics can be easily separated in the frequency domain.

Here we are interested in the scattering properties of the fundamental mode. In the positive direction (corresponds to high transmission), the transmission is defined as $S_{21} = t_0$. Similarly, the scattering parameter S_{12} (corresponds to the transmission in the negative direction) is computed by switching the initial phase of the two resonators, i.e., $\phi_1 \leftrightarrow \phi_2$. Two key parameters are analyzed to evaluate the performance of the system: the isolation factor $20\log|S_{21}/S_{12}|$ and the insertion loss $IL = -20\log S_{21}$, where the isolation factor measures the efficiency of one-way isolation of the acoustic waves and the insertion loss calculates the attenuation of the transmission in the positive direction.

Figure 2 shows contour plots of the two key performance parameters as a function of incident frequency f and modulation depth m obtained from the analytic model. It can be seen that the isolation factor can be as high as 50 dB, and two bands with large isolation are created by applying spatiotemporal modulation on the system. The separation of the two bands are larger by increasing the modulation depth, with smaller insertion loss. On the other hand, a higher isolation factor is achieved with small m near resonance frequency, but is accompanied by larger insertion loss. This indicates that efficient nonreciprocal transmission can be obtained by suitably choosing the modulation depth and incident frequency. To realize nonreciprocal transmission, the modulation depth m is chosen to be 0.235, marked by points A and B, to yield a relatively small insertion loss. The incident frequency, isolation factor and insertion loss at points A and B are 1.84 kHz, 35.1 dB, 11.7 dB and 2.14 kHz, 23.5 dB, 13.3 dB, respectively. This performance incorporates the balance of isolation factor and insertion loss, and larger isolation can be achieved by choosing a smaller m but at the expense of higher reflection.

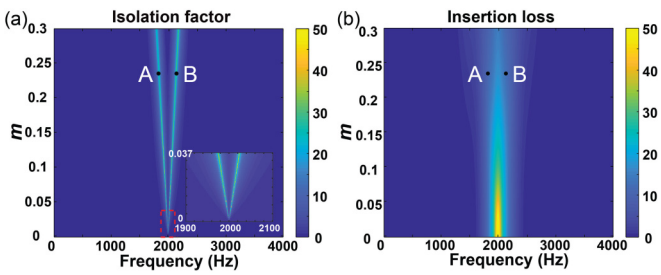

FIG. 2. (a) Isolation factor and (b) insertion loss of the cascaded resonator system under spatiotemporal modulation. The inset shows the zoom-in view of the dotted region. The points A and B mark the parameters implemented in numerical simulations.

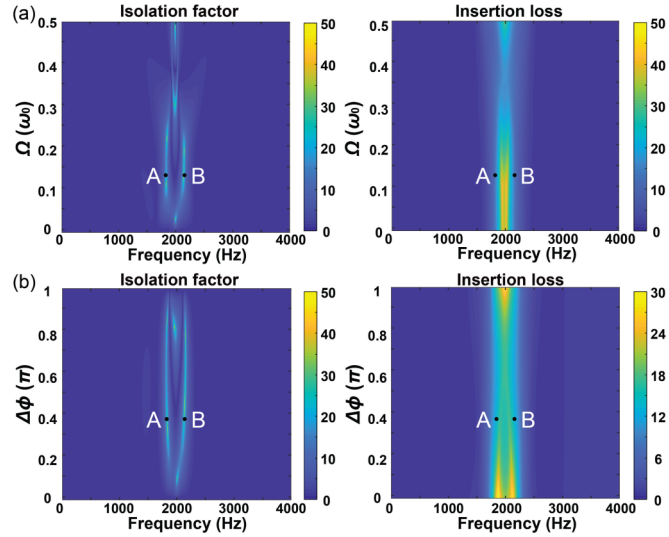

FIG. 3. Effect of modulation frequency (Ω) and initial phase difference ($\Delta\phi$) on the performance of the system. The ranges of Ω and $\Delta\phi$ are set to be $[0\ 0.5\omega_0]$ and $[0\ \pi]$, respectively. The marked points A and B are consistent with those shown in Fig. 2.

To study the effect of modulation frequency and initial phase difference, we also plot the isolation factor and insertion loss by varying Ω and $\Delta\phi$ from 0 to $0.5\omega_0$ and 0 to π, respectively. Other modulation parameters are kept constant and are $m = 0.235$ and $d = 4.29$ cm. The results are summarized in Fig. 3. It can be seen that their effect on the performance of the system is more complex than the modulation depth. Generally, since high insertion loss is observed near the resonance frequency, the strategy is to choose Ω and $\Delta\phi$ such that the bands with high nonreciprocity are away from the resonance frequency. As illustrated by the marked points A and B, the parameters implemented in numerical simulations are carefully chosen by balancing isolation factor and insertion loss. The transmission for the fundamental mode with $\Omega = 0.125\omega_0$ and $\Delta\phi = 0.4\pi$ is shown in Fig. 4, with the strong nonreciprocal transmission region marked by the

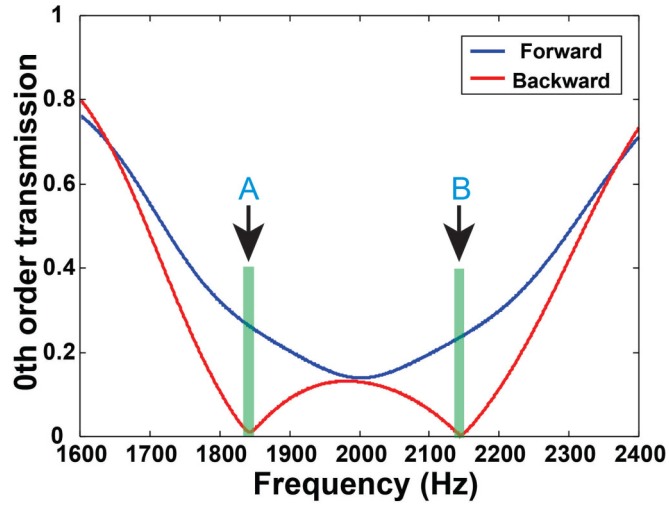

FIG. 4. Nonreciprocal transmission within two frequency bands using time-modulated resonators. The shaded stripes denote nonreciprocal transmission for the zeroth order wave at points A and B.

shaded stripes. It can be seen that the 0th order transmission is greatly suppressed in the negative direction within the two frequency bands, therefore yielding strong one-way isolation.

III. SIMULATION

The analytic model is then verified with two-dimensional (2D) FDTD simulations. The background medium is assumed to be air with density $\rho_0 = 1.2$ kg/m^3 and velocity $c_0 = 343$ m/s. The width and height of the neck are 1.0 and 1.2 mm, respectively and the dimension of the cavity is 34 mm by 6.6 mm, yielding a resonance frequency of 2000 Hz. The height of the waveguide is 18 mm to give a quality factor of 3.6. It should be pointed out that since the theory does not restrict the dimensions of the resonators and the waveguide, the actual geometry can be tuned as long as the resonance frequency and quality factor of the entire system meet the theoretical requirements.

The FDTD simulation directly reflects the physical system given above, i.e., the actual geometry of the resonators and the waveguide is simulated without any effective property approximations. The simulation incorporates temporal modulation by updating the top boundary position of the cavities in each time step. Since m is small, the required modulation in Eq. (3) is approximated by $h_{1,2}(t) = h_0 + m\cos(\Omega t - \phi_{1,2})$, where h_0 and $h_{1,2}(t)$ are the heights of the cavities in the static case and under dynamic modulation. A sine wave with targeted frequency is incident on one end of the waveguide and a perfect matched layer (PML) is used on the other end of the waveguide to minimize reflections [25]. The transmitted signals at the end of the waveguide are recorded and zero padding and a Hamming window are further applied. The transmission of different frequencies are then obtained by performing an inverse Fourier transform of the resulted signals.

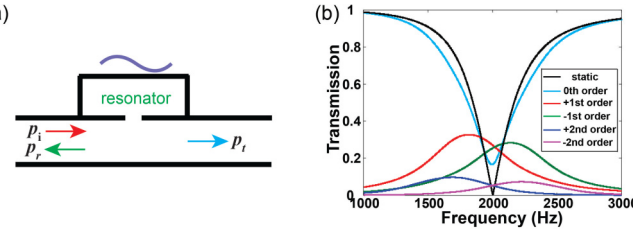

FIG. 5. Transmission through a single time-modulated resonator. (a) Sketch of the system. (b) Analytically calculated transmission in the static case and under time modulation of different modes.

First, we consider the case of a single time-modulated resonator. The parameters are the same with the two-resonator case. The schematic diagram of the system is shown in Fig. 5(a), the corresponding transmission spectrum of different harmonics is shown in Fig. 5(b). It can be seen that with the spatiotemporal modulation, the energy of the 0th mode is partially converted to the ±1st and ±2nd modes near the resonance frequency. The corresponding FDTD simulation results are plotted in Fig. 6 at different frequencies. Good agreement between the theory and simulations can be observed: the conversion to the ±1st modes is clear and the transmission of each individual mode matches well with each other at various frequencies. The conversion from fundamental mode to other harmonics is more efficient below the resonance frequency and is consistent with the results in Fig. 6. Moreover, the amplitude of the higher order harmonics are much less than the 0th, ±1st, and ±2nd modes and is generally below 0.015, which validates the approximation of truncation under weak modulation.

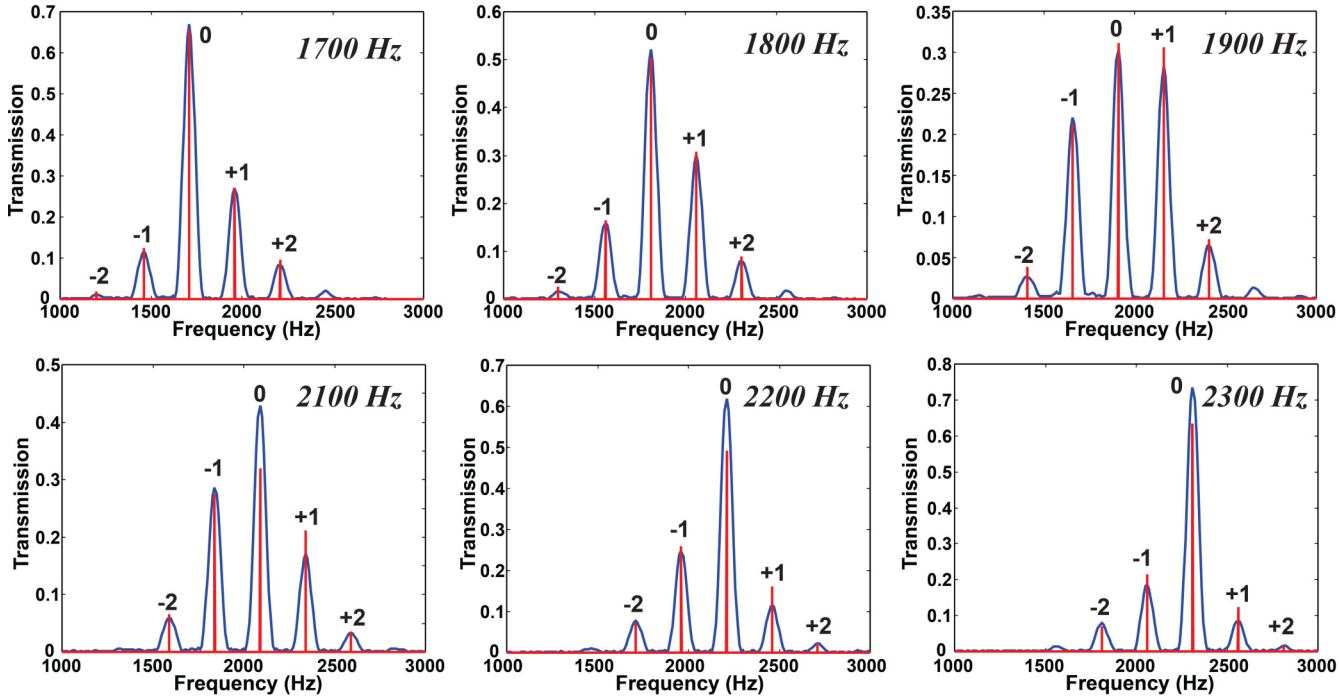

FIG. 6. Comparison of the transmission of different modes in theory and simulations at different frequencies. The harmonic orders are labeled in the peaks. Blue curve: Results obtained by FDTD simulations. Red curve: Theoretically predicted transmission at 0th, ±1st, and ±2nd modes, higher order harmonics are truncated in derivation.

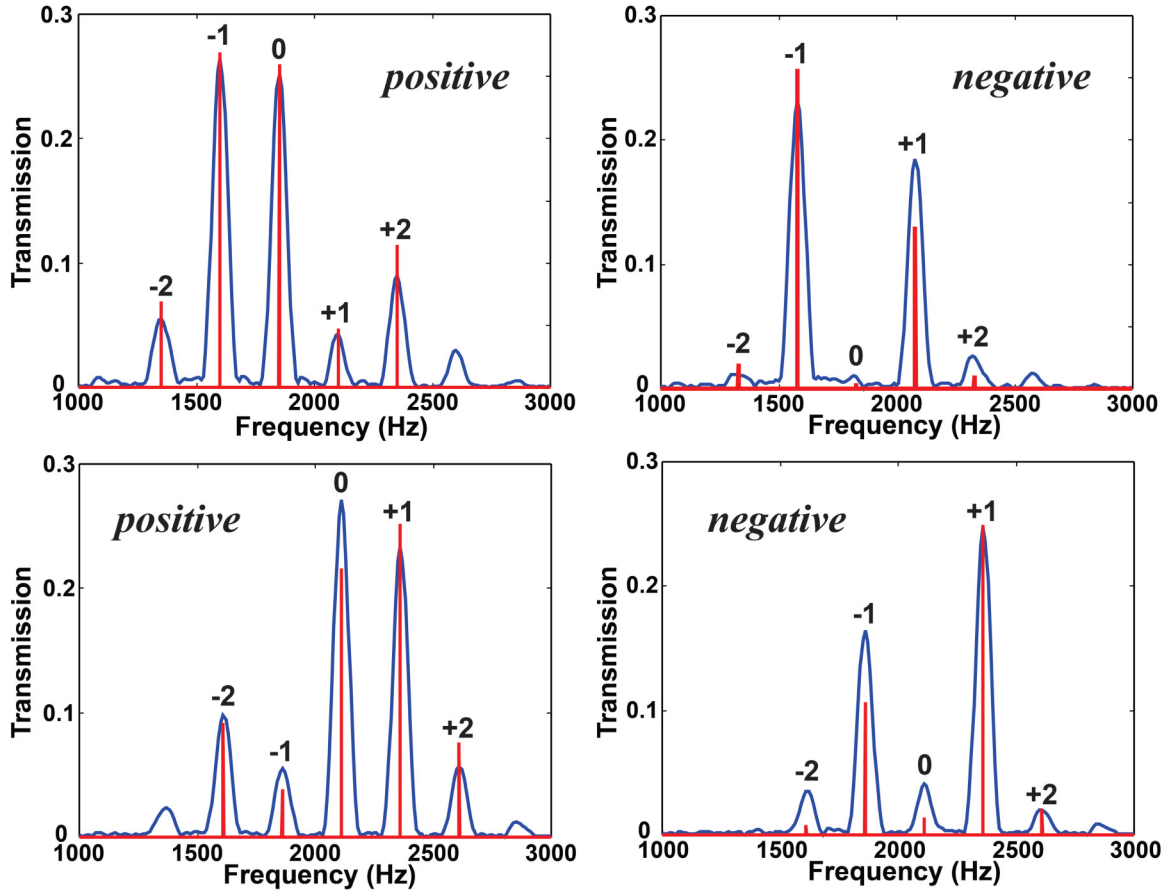

FIG. 7. Simulated results of nonreciprocal transmission in the two time-modulated resonators system. The harmonic orders are labeled in the peaks. Top and bottom panels show the results at 1.84 and 2.14 kHz, respectively. Blue curve and red curve represent results from simulations and theory, respectively. The transmission of the fundamental mode is vastly different in opposite directions.

Next, we study nonreciprocity by performing two sets of simulations by switching the order of the resonators. The two resonators have an initial phase difference of $\Delta\phi = 0.4\pi$ under modulation and the results are depicted in Fig. 7. In the positive direction, the transmission of the fundamental mode (1.84 and 2.14 kHz) is high, while in the negative direction, the 0th order transmission is extremely low. A clear nonreciprocal transmission is therefore observed, the isolation factor in simulation is 27.7 and 16.4 dB for 1.84 and 2.14 kHz, respectively. This isolation is smaller than theoretical predictions and can be attributed to the neglect of higher order harmonics in the analytic approach and limited spatial and temporal resolution in the FDTD simulations. Remarkably, it can be observed from simulations that the transmission at higher order harmonics ($\pm$2nd modes) are more profound in the two-resonator system, which is because of the interaction between the two resonators and conversion among different modes. Better agreement may be achieved by taking the $\pm$3rd modes into consideration in the analytic approach.

IV. DISCUSSION AND CONCLUSION

To conclude, we have demonstrated nonreciprocal acoustic transmission in cascaded resonators based on spatiotemporal modulation in theory and numerical simulations. An analytic approach based on mode expansion is developed and strong nonreciprocity is manifested in a two-resonator system with spatially biased modulation phases. The time modulation and initial phase difference impart a directional bias to the system such that for incoming waves in the negative direction, most of the energy of the fundamental harmonic is converted to the higher-order harmonics. On the other hand, some of the energy of the higher-order harmonics generated by the first resonator is converted back to the fundamental mode at the second resonator in the positive direction and therefore strong nonreciprocity is achieved.

The proposed approach for realizing nonreciprocity features a high isolation factor and compact geometry, with an overall size around a quarter wavelength. Our FDTD simulations with physically realistic structures indicate that the approach can be readily applied to real scenarios with proper modulation techniques. For example, the required dynamic modulation of the resonators can be realized by connecting the back wall of the cavities to mechanical vibrators. To optimize performance, the geometries of the resonators and the waveguide can be tuned since the theory does not pose any restrictions on the real system. For example, the height of the cavities can be adjusted to larger values for better accuracy or smaller values for higher modulation depth. We also note that the analytic approach outlined here can be extended to systems consisting of more than two resonators. With more degrees of freedom offered by additional resonators,

nonreciprocity may be more profound and other functionalities may be achieved. Higher order harmonics can also be included in the theory to yield a more accurate result. Such compact systems may also be integrated into larger scales to form topological insulators [11,12,26]. It is hoped that this work can be useful for the realization of compact nonreciprocal acoustic devices and will benefit areas including imaging, sensing, and noise control.

ACKNOWLEDGMENTS

This work was supported by a Multidisciplinary University Research Initiative grant from the Office of Naval Research (Grant No. N00014-13-1-0631) and an Emerging Frontiers in Research and Innovation grant from the National Science Foundation (Grant No. 1641084). C.S. wishes to thank Dr. Q. Zhan for helpful discussions on the simulations.

[1] J. D. Adam, L. E. Davis, G. F. Dionne, E. F. Schloemann, and S. N. Stitzer, IEEE Trans. Microwave Theory Tech. **50**, 721 (2002).
[2] D. L. Sounas and A. Alù, Nat. Photon. **11**, 774 (2017).
[3] L. Lu, J. D. Joannopoulos, and M. Soljačić, Nat. Photon. **8**, 821 (2014).
[4] M. C. Rechtsman, J. M. Zeuner, Y. Plotnik, Y. Lumer, D. Podolsky, F. Dreisow, S. Nolte, M. Segev, and A. Szameit, Nature (London) **496**, 196 (2013).
[5] R. Fleury, D. Sounas, M. R. Haberman, and A. Alù, Acoust. Today **11**, 14 (2015).
[6] B. Liang, B. Yuan, and J.-C. Cheng, Phys. Rev. Lett. **103**, 104301 (2009).
[7] B. Liang, X. Guo, J. Tu, D. Zhang, and J. Cheng, Nat. Mater. **9**, 989 (2010).
[8] N. Boechler, G. Theocharis, and C. Daraio, Nat. Mater. **10**, 665 (2011).
[9] B.-I. Popa and S. A. Cummer, Nat. Commun. **5**, 3398 (2014).
[10] Z. Yang, F. Gao, X. Shi, X. Lin, Z. Gao, Y. Chong, and B. Zhang, Phys. Rev. Lett. **114**, 114301 (2015).
[11] R. Fleury, A. B. Khanikaev, and A. Alù, Nat. Commun. **7**, 11744 (2016).
[12] Y. Ding, Y. Peng, Y. Zhu, X. Fan, J. Yang, B. Liang, X. Zhu, X. Wan, and J. Cheng, Phys. Rev. Lett. **122**, 014302 (2019).
[13] K. Fang, Z. Yu, and S. Fan, Phys. Rev. Lett. **108**, 153901 (2012).
[14] K. Fang, Z. Yu, and S. Fan, Nat. Photon. **6**, 782 (2012).
[15] R. Fleury, D. L. Sounas, C. F. Sieck, M. R. Haberman, and A. Alù, Science **343**, 516 (2014).
[16] N. A. Estep, D. L. Sounas, and A. Alù, Nat. Phys. **10**, 923 (2014).
[17] Y. Hadad, D. L. Sounas, and A. Alù, Phys. Rev. B **92**, 100304(R) (2015).
[18] R. Fleury, D. L. Sounas, and A. Alù, Phys. Rev. B **91**, 174306 (2015).
[19] N. Reiskarimian and H. Krishnaswamy, Nat. Commun. **7**, 11217 (2016).
[20] G. Trainiti and M. Ruzzene, New J. Phys. **18**, 083047 (2016).
[21] H. Nassar, H. Chen, A. Norris, M. Haberman, and G. Huang, Proc. R. Soc. London Ser. A **473**, 20170188 (2017).
[22] D. Torrent, O. Poncelet, and J.-C. Batsale, Phys. Rev. Lett. **120**, 125501 (2018).
[23] K. Yi, M. Collet, and S. Karkar, Phys. Rev. B **98**, 054109 (2018).
[24] Y. Cheng, J. Xu, and X. J. Liu, Phys. Rev. B **77**, 045134 (2008).
[25] X. Yuan, D. Borup, J. Wiskin, M. Berggren, R. Eidens, and S. Johnson, IEEE Trans. UFFC **44**, 816 (1997).
[26] A. Alù, Nat. Phys. **13**, 1038 (2017).